

LETTER • OPEN ACCESS

Doping-dependent fixed charges in SiC/SiO₂ structure

To cite this article: Kyota Mikami *et al* 2025 *Appl. Phys. Express* **18** 034002

View the [article online](#) for updates and enhancements.

You may also like

- [Ampere-class double pulse testing of half-inch H-terminated diamond MOSFET chip](#)
Keita Takaesu, Daisuke Sano, Iku Ota *et al.*
- [Influence of fixed charges and trapped electrons on free electron mobility at 4H-SiC\(0001\)/SiO₂ interfaces with gate oxides annealed in NO or POCl₃](#)
Koji Ito, Hajime Tanaka, Masahiro Horita *et al.*
- [Density and energy level of near-interface trap estimated by analysis of threshold voltage shift due to positive bias stress in GaN planar MOSFETs with SiO₂ gate dielectric](#)
Yuki Ichikawa, Katsunori Ueno, Tsurugi Kondo *et al.*



UNITED THROUGH SCIENCE & TECHNOLOGY

 **The Electrochemical Society**
Advancing solid state & electrochemical science & technology

**248th
ECS Meeting**
Chicago, IL
October 12-16, 2025
Hilton Chicago

**Science +
Technology +
YOU!**

**Abstract submission
deadline extended:
April 11, 2025**

SUBMIT NOW



Doping-dependent fixed charges in SiC/SiO₂ structure

Kyota Mikami^{*}, Mitsuaki Kaneko, and Tsunenobu Kimoto

Department of Electronic Science and Engineering, Kyoto University, Nishikyo, Kyoto 615-8510, Japan

^{*}E-mail: mikami@semicon.kuee.kyoto-u.ac.jp

Received January 16, 2025; revised February 3, 2025; accepted February 12, 2025; published online March 6, 2025

Doping-dependent fixed charges were found in SiC/SiO₂ structures through a study on threshold voltage in both n- and p-channel SiC metal-oxide-semiconductor field-effect transistors (MOSFETs) with various body doping concentrations. Positive fixed charges increase for the p-body (n-channel) devices and negative fixed charges increase for the n-body (p-channel) devices, both of which retard the increase of threshold voltage in MOSFETs with increasing the body doping. © 2025 The Author(s). Published on behalf of The Japan Society of Applied Physics by IOP Publishing Ltd

Silicon carbide (SiC) is one of the most promising semiconductor materials for highly efficient power devices and high-temperature operational devices owing to its superior material properties, such as high critical electric field and wide bandgap.^{1–3)} Moreover, the availabilities of high-quality large-diameter wafers, high-quality epitaxial growth, and wide-range doping control of both n- and p-type in SiC⁴⁾ are great advantages for electronic device applications. SiC power metal-oxide-semiconductor field-effect transistors (MOSFETs) are currently available as next-generation power devices, and SiC complementary MOS (CMOS) devices have attracted much attention for high-temperature operating ICs.^{5–7)} So far, the SiC MOS community has mainly focused on channel mobility in terms of mobility improvement^{8–14)} and elucidation of carrier scattering mechanism in the inversion layer.^{15–20)} As for threshold voltage (V_{TH}), instability at high gate biases and elevated temperatures^{21–24)} has been the main subject of study. Although precise control of threshold voltage by body doping is essential, especially for CMOS applications, such studies have been very limited for both n- and p-channel SiC MOSFETs.

G. Ortiz et al. reported that the experimental V_{TH} for n-channel SiC MOSFETs with lightly-doped bodies was close to the theoretical V_{TH} .²⁵⁾ On the other hand, the experimental V_{TH} for heavily-doped MOSFETs showed a negative shift from the theoretical V_{TH} , which cannot be explained by electron trapping at the interface states. They concluded that the negative V_{TH} shift is caused by positive fixed charges of which the density depends on the acceptor concentration of p-body. However, it is known that the density of fixed charges is independent of body doping concentration in Si MOSFETs.^{26,27)} Therefore, in this study, the authors investigated the body doping dependence of threshold voltage and fixed charges for both n- and p-channel SiC MOSFETs not only for power MOSFET applications but also for CMOS applications.

The starting materials were a p-type 4H-SiC (0001) epilayer for n-channel MOSFETs and an n-type epilayer for p-channel MOSFETs. The body doping concentrations (N_{Body}) were 1×10^{15} – 4×10^{17} cm⁻³ for p-body and 5×10^{15} – 2×10^{18} cm⁻³ for n-body, controlled either by epitaxial growth or by ion implantation. The source and drain regions were formed by high-dose implantation of Al⁺

for p⁺ regions and P⁺ for n⁺ regions. The gate oxide was formed by dry oxidation at 1300 °C for 20 min, followed by NO annealing^{28,29)} at 1250 °C for 70 min, resulting in an oxide thickness of about 32 nm. The channel length, width, and gate metal were 100 μm, 50–170 μm, and Al, respectively. A more detailed process is presented in our earlier report.³⁰⁾

In general, an experimental threshold voltage is determined by an extrapolated intercept of the linear portion of the gate characteristics at low drain voltages. In SiC MOSFETs, however, such experimental threshold voltage cannot be uniquely determined because a linear portion of the gate characteristics is hardly observed due to the high density of interface states. Therefore, the experimental threshold voltage of the fabricated MOSFETs was determined by using the total carrier density obtained by Split C – V measurements (N_{split}). Figure 1 shows the N_{split} as a function of the gate voltage (V_{GS}) for the n- and p-channel SiC MOSFETs. The N_{split} – V_{GS} characteristics shifted towards the negative V_{GS} direction for the p-channel devices and the positive V_{GS} direction for the n-channel devices with increasing N_{Body} . Note that the slopes of N_{split} – V_{GS} characteristics are almost identical for all the MOSFETs, corresponding to the oxide capacitance. The experimental threshold voltage was defined as the gate voltage at $N_{split} = 1 \times 10^{11}$ cm⁻².

Figure 2 depicts the body doping dependence of threshold voltage in SiC MOSFETs. The theoretical threshold voltage was calculated using the surface potential obtained by solving Poisson's equation where the free carrier density was 1×10^{11} cm⁻². In the low N_{Body} region ($< 10^{17}$ cm⁻³), a slightly negative V_{TH} shift was observed for both n- and p-channel devices. In contrast, in the high N_{Body} region ($> 10^{17}$ cm⁻³), the n-channel device with $N_{Body} = 4 \times 10^{17}$ cm⁻³ showed a negative V_{TH} shift of 4.3 V, while the p-channel device with $N_{Body} = 2 \times 10^{18}$ cm⁻³ showed a positive V_{TH} shift of 3.9 V.

The density of effective fixed charges (Q_{eff}), consisting of the density of trapped electrons/holes and fixed charges, was extracted from the threshold voltage shift, denoted by $Q_{eff}(V_{TH})$, and the results are shown in Fig. 3(a). Here, Q_{eff} was also extracted from the flatband voltage shift of MOS capacitors fabricated on the same chip as the MOSFETs, denoted by $Q_{eff}(V_{FB})$. Positive Q_{eff} increases for the p-body (n-channel) devices and negative Q_{eff} increases for the n-body (p-channel) devices, which are observed for both



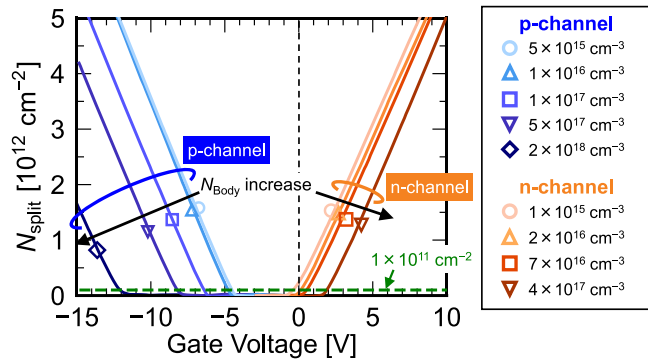


Fig. 1. Total carrier density obtained by Split C - V measurements as a function of the gate voltage for both n- and p-channel 4H-SiC (0001) MOSFETs with various body doping concentrations (N_{Body}).

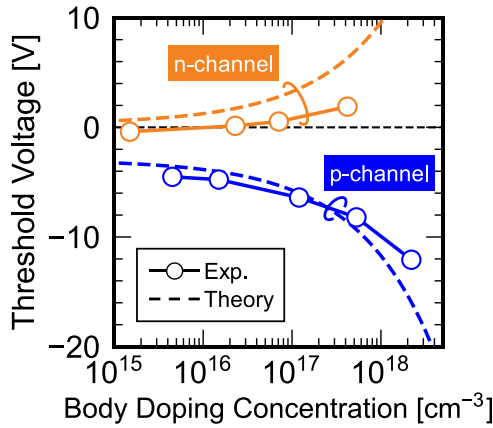


Fig. 2. Body doping dependence of threshold voltage (V_{TH}) for both n- and p-channel 4H-SiC (0001) MOSFETs. The experimental V_{TH} negatively shifted for both MOSFETs with lightly-doped bodies ($<10^{17} \text{ cm}^{-3}$). In contrast, the MOSFETs with heavily-doped bodies ($>10^{17} \text{ cm}^{-3}$) showed a negative V_{TH} shift for the n-channel devices and a positive V_{TH} shift for the p-channel devices.

$Q_{\text{eff}}(V_{\text{TH}})$ and $Q_{\text{eff}}(V_{\text{FB}})$. $|Q_{\text{eff}}|$ reached a high density of more than $2 \times 10^{12} \text{ cm}^{-2}$ for the heavily-doped devices. $Q_{\text{eff}}(V_{\text{TH}})$ extracted from n-channel MOSFETs exhibited almost the same N_{Body} dependence as $Q_{\text{eff}}(V_{\text{FB}})$ extracted from p-type MOS capacitors. A similar trend was also observed for $Q_{\text{eff}}(V_{\text{TH}})$ extracted from p-channel MOSFETs and $Q_{\text{eff}}(V_{\text{FB}})$ extracted from n-type MOS capacitors. This

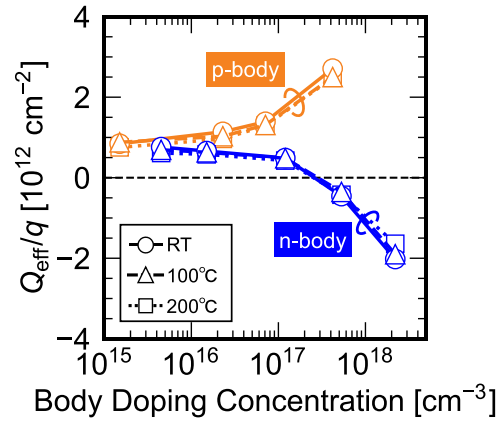


Fig. 4. Relationship between the body doping concentration and density of effective fixed charges (Q_{eff}) extracted from flatband voltage shifts of both n- and p-type MOS capacitors at RT, 100 °C, and 200 °C.

phenomenon can be interpreted as follows. Taking the p-body devices as an example, the surface Fermi level at the threshold and flatband voltages are located near the conduction and valence band edges, as shown in Figs. 3(b) and 3(c), respectively. Here, $Q_{\text{eff}}(V_{\text{TH}})$ is the total density of fixed charges and trapped electrons, whereas $Q_{\text{eff}}(V_{\text{FB}})$ is the total density of fixed charges and trapped holes because deep interface states have a large time constant and carriers trapped at such interface states act as fixed charges.⁴⁾ The experimental result that $Q_{\text{eff}}(V_{\text{TH}})$ is similar to $Q_{\text{eff}}(V_{\text{FB}})$ at a given N_{Body} indicates that the influence of trapped electrons/holes on Q_{eff} is limited (less than $5 \times 10^{11} \text{ cm}^{-2}$) and that the majority of effective fixed charges consists of the fixed charges. In other words, Fig. 3 implies that the density of fixed charges in SiC/SiO₂ structures strongly depends on the body conduction type and doping concentration.

To further obtain verification of the existence of doping-dependent fixed charges in SiC/SiO₂ structures, $Q_{\text{eff}}-N_{\text{Body}}$ relations were investigated at high temperatures where emission of trapped carriers from the interface states is enhanced. Figure 4 shows the relationship between the body doping concentration and Q_{eff} extracted from the flatband voltage shift of both n- and p-type MOS capacitors at RT, 100 °C, and 200 °C. The $Q_{\text{eff}}-N_{\text{Body}}$ relations at 100 and 200 °C are comparable to that at RT, implying the

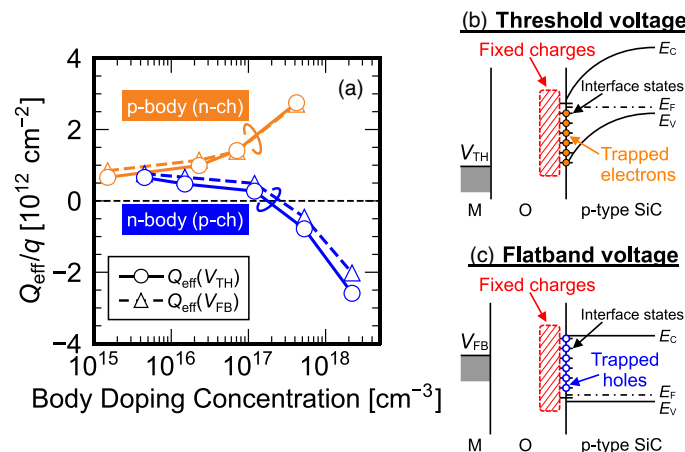


Fig. 3. (a) Relationship between the body doping concentration and density of effective fixed charges (Q_{eff}) extracted from threshold voltage (V_{TH}) and flatband voltage (V_{FB}) shifts. Figures (b) and (c) show the band diagrams of p-body devices at the threshold and flatband voltages, respectively.

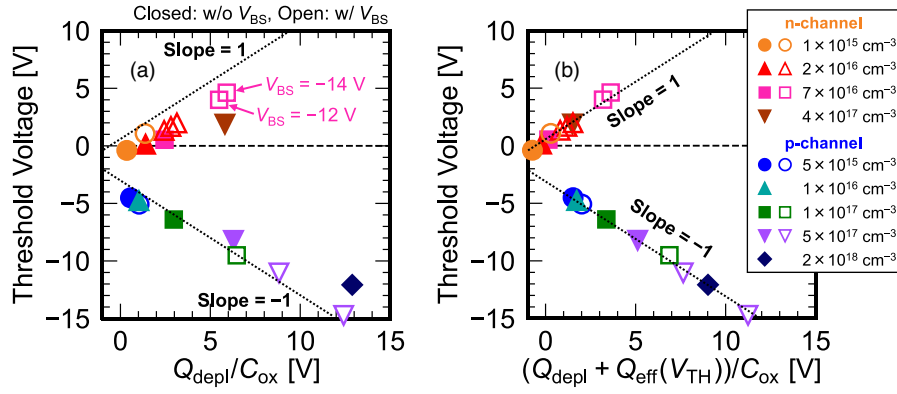


Fig. 5. Threshold voltages with and without body biasing (V_{BS}) as a function of (a) $Q_{\text{depl}}/C_{\text{ox}}$ and (b) $(Q_{\text{depl}} + Q_{\text{eff}}(V_{\text{TH}}))/C_{\text{ox}}$, where Q_{depl} is the depletion charge density, $Q_{\text{eff}}(V_{\text{TH}})$ is the density of effective fixed charges extracted from threshold voltage shift, and C_{ox} is the oxide capacitance. The applied body biases were negative for the n-channel MOSFETs and positive for the p-channel MOSFETs.

existence of doping-dependent fixed charges and that the contribution of trapped carriers is very small ($<5 \times 10^{11} \text{ cm}^{-2}$).

Figure 5(a) depicts the threshold voltage as a function of the depletion charge density (Q_{depl}) divided by the oxide capacitance (C_{ox}). The threshold voltage of MOSFETs is given by³¹⁾

$$V_{\text{TH}} = \phi_{\text{Gate}} - \phi_{\text{S}} \pm 2|\psi_{\text{B}}| \pm \frac{\sqrt{2\varepsilon_{\text{S}}qN_{\text{Body}}(2|\psi_{\text{B}}| \mp V_{\text{BS}})}}{C_{\text{ox}}} + \frac{Q_{\text{eff}}}{C_{\text{ox}}}, \quad (1)$$

where ϕ_{Gate} is the gate work function, ϕ_{S} is the semiconductor work function, ψ_{B} is the bulk potential, ε_{S} is the dielectric constant of a semiconductor, q is the elementary charge, and V_{BS} is a body bias (usually 0 V unless intentionally applied). The upper and lower signs refer to n- and p-channel MOSFETs, respectively. Here, $\sqrt{2\varepsilon_{\text{S}}qN_{\text{Body}}(2|\psi_{\text{B}}| \mp V_{\text{BS}})}$ is the depletion charge density. If Q_{eff} is almost negligible or their density is independent of N_{Body} like Si MOSFETs, threshold voltages with or without body biasing plotted against $Q_{\text{depl}}/C_{\text{ox}}$ should have a slope of +1 for n-channel devices and -1 for p-channel devices. As shown in Fig. 5(a), however, the relationship with such a slope was not observed for both MOSFETs. In other words, $Q_{\text{depl}}/C_{\text{ox}}$ does not uniquely determine the threshold voltage in SiC MOSFETs. Taking the n-channel MOSFETs as an example, the threshold voltage was 1.9 V for the $N_{\text{Body}} = 4 \times 10^{17} \text{ cm}^{-3}$ device without body biasing and 4.0–4.6 V for the $N_{\text{Body}} = 7 \times 10^{16} \text{ cm}^{-3}$ device with body biasing of -12 to -14 V even though these devices had the same $Q_{\text{depl}}/C_{\text{ox}}$ of about 6 V [see Fig. 5(a)]. To consider the influence of fixed charges on the $V_{\text{TH}}-Q_{\text{depl}}/C_{\text{ox}}$ relation, the threshold voltages were plotted against $(Q_{\text{depl}} + Q_{\text{eff}}(V_{\text{TH}}))/C_{\text{ox}}$, in Fig. 5(b). Note that the $Q_{\text{eff}}(V_{\text{TH}})$ of the devices with body biasing is the $Q_{\text{eff}}(V_{\text{TH}})$ extracted for the same N_{Body} devices without body biasing. Since $V_{\text{TH}}-(Q_{\text{depl}} + Q_{\text{eff}}(V_{\text{TH}}))/C_{\text{ox}}$ relations with a slope of +1 for the n-channel devices and -1 for the p-channel devices were observed, the body doping and body bias dependence of threshold voltage in both n- and p-channel SiC MOSFETs can be predicted by considering doping-dependent fixed charges.

In conclusion, the authors investigated the body doping dependence of threshold voltage in both n- and p-channel SiC MOSFETs and found doping-dependent fixed charges, which have not been reported in Si/SiO₂ structures. As the body doping increases, positive fixed charges increase for the p-

body devices and negative fixed charges increase for the n-body devices. The $Q_{\text{eff}}-N_{\text{Body}}$ relations do not depend on temperatures, supporting the existence of doping-dependent fixed charges in SiC/SiO₂ structures. The density of fixed charges in SiC/SiO₂ structures reached as high as $\sim 10^{12} \text{ cm}^{-2}$, while that in Si/SiO₂ structures is less than 10^{11} cm^{-2} achieved by the appropriate process conditions.³²⁾ Since such a high density of fixed charges in SiC/SiO₂ structures would also cause significant degradation of drift mobility in the inversion layer, further investigations are required to reveal the origin and reduce the density.

Acknowledgments This work was supported in part by the Block-Gift Program of Ii-VI Foundation, in part by the JSPS KAKENHI Grant No. JP21H05003, and in part by the JST ALCA-Next Program Number JPMJAN24E5.

ORCID iDs Kyota Mikami <https://orcid.org/0000-0002-1922-6064> Mitsuaki Kaneko <https://orcid.org/0000-0001-5629-0105> Tsunenobu Kimoto <https://orcid.org/0000-0002-6649-2090>

- 1) P. G. Neudeck, R. S. Okojie, and L. Y. Chen, *Proc. IEEE* **90**, 1065 (2002).
- 2) B. J. Baliga, *Fundamentals of Power Semiconductor Devices* (Springer, Berlin, 2008).
- 3) T. Kimoto and H. Watanabe, *Appl. Phys. Express* **13**, 120101 (2020).
- 4) T. Kimoto and J. A. Cooper, *Fundamentals of Silicon Carbide Technology* (Wiley, Singapore, 2014).
- 5) S. Ryu, K. T. Korngay, J. A. Cooper Jr., and M. R. Melloch, *IEEE Electron Device Lett.* **18**, 194 (1997).
- 6) M. Okamoto, T. Yatsuo, K. Fukuda, and H. Okumura, *Jpn. J. Appl. Phys.* **48**, 04C087 (2009).
- 7) M. Barlow, S. Ahmed, A. M. Francis, and H. A. Mantooth, *IEEE Trans. Power Electron.* **34**, 11191 (2019).
- 8) H. Yano, T. Hirao, T. Kimoto, H. Matsunami, K. Asano, and Y. Sugawara, *IEEE Electron Device Lett.* **20**, 611 (1999).
- 9) G. Y. Chung et al., *IEEE Electron Device Lett.* **22**, 176 (2001).
- 10) D. Okamoto, H. Yano, K. Hirata, T. Hatayama, and T. Fuyuki, *IEEE Electron Device Lett.* **31**, 710 (2010).
- 11) D. J. Lichtenwalner, L. Cheng, S. Dhar, A. Agarwal, and J. W. Palmour, *Appl. Phys. Lett.* **105**, 182107 (2014).
- 12) T. Hosoi, Y. Katsu, K. Moges, D. Nagai, M. Sometani, H. Tsuji, T. Shimura, and H. Watanabe, *Appl. Phys. Express* **11**, 091301 (2018).
- 13) K. Tachiki, K. Mikami, K. Ito, M. Kaneko, and T. Kimoto, *Appl. Phys. Express* **15**, 071001 (2022).
- 14) K. Mikami, M. Kaneko, and T. Kimoto, *IEEE Electron Device Lett.* **45**, 1113 (2024).
- 15) V. Uhnevionak, A. Burenkov, C. Strenger, G. Ortiz, E. Bedel-Pereira, and V. Mortet, *IEEE Trans. Electron Devices* **62**, 2562 (2015).
- 16) M. Sometani, T. Hosoi, H. Hirai, T. Hatakeyama, S. Harada, H. Yano, T. Shimura, H. Watanabe, Y. Yonezawa, and H. Okumura, *Appl. Phys. Lett.* **115**, 132102 (2019).

- 17) M. Noguchi, T. Iwamatsu, H. Amishiro, H. Watanabe, K. Kita, and N. Miura, *Jpn. J. Appl. Phys.* **59**, 051006 (2020).
- 18) H. Hirai, T. Hatakeyama, M. Sometani, M. Okamoto, S. Harada, H. Okumura, and H. Yamaguchi, *Appl. Phys. Lett.* **117**, 042101 (2020).
- 19) S. Das, T. Isaacs-Smith, A. Ahyi, M. A. Kuroda, and S. Dhar, *J. Appl. Phys.* **130**, 225701 (2021).
- 20) K. Ito, H. Tanaka, M. Horita, J. Suda, and T. Kimoto, *Appl. Phys. Express* **17**, 081003 (2024).
- 21) A. J. Lelis, R. Green, D. B. Habersat, and M. El, *IEEE Trans. Electron Devices* **62**, 316 (2015).
- 22) H. Yano, N. Kanafuji, A. Osawa, T. Hatayama, and T. Fuyuki, *IEEE Trans. Electron Devices* **62**, 324 (2015).
- 23) T. Aichinger, G. Rescher, and G. Pobegen, *Microelectron. Reliab.* **80**, 68 (2018).
- 24) K. Puschkarsky, T. Grasser, T. Aichinger, W. Gustin, and H. Reisinger, *IEEE Trans. Electron Devices* **66**, 4604 (2019).
- 25) G. Ortiz, C. Strenger, V. Uhnevionak, A. Burenkov, A. J. Bauer, P. Pichler, F. Cristiano, E. Bedel-Pereira, and V. Mortet, *Appl. Phys. Lett.* **106**, 062104 (2015).
- 26) A. S. Grove, B. E. Deal, E. H. Snow, and C. T. Sah, *Solid State Electron.* **8**, 145 (1965).
- 27) B. E. Deal, M. Sklar, A. S. Grove, and E. H. Snow, *J. Electrochem. Soc.* **114**, 266 (1967).
- 28) H. Li, S. Dimitrijević, H. B. Harrison, and D. Sweatman, *Appl. Phys. Lett.* **70**, 2028 (1997).
- 29) G. Y. Chung, C. C. Tin, J. R. Williams, K. McDonald, M. Di Ventra, S. T. Pantelides, L. C. Feldman, and R. A. Weller, *Appl. Phys. Lett.* **76**, 1713 (2000).
- 30) K. Mikami, K. Tachiki, K. Ito, and T. Kimoto, *Appl. Phys. Express* **15**, 036503 (2022).
- 31) S. M. Sze and K. K. Ng, *Physics of Semiconductor Devices* (Wiley, Hoboken, New Jersey, 2007) 3rd ed.
- 32) S. I. Raider and A. Berman, *J. Electrochem. Soc.* **125**, 629 (1978).